Control of a Novel Integrated Radial-Axial Magnetic Bearing

Erik Fleischer*, Stefan Tröger and Wilfried Hofmann
Technische Universiät Dresden
Dresden, Germany

Abstract

An important application area of magnetic bearings is machinery running in vacuum. Examples include vacuum pumps, flywheels and spin wheels for space craft. Here even small rotor losses can overheat the rotor because of the low heat transfer in vacuum. Therefore this project aims at realizing a magnetic suspension with minimal rotor losses.

Thus a novel magnetic bearing structure has been developed. It can generate both radial and axial forces and employs a minimal number of poles and soft magnetic composites as iron core material for minimal losses.

This paper presents the new bearing structure and a control strategy for it. The designed controller is verified in simulations and first experimental results are presented as well.

1 Introduction

Active magnetic bearings have become an attractive choice for applications with high demands on the bearings like long service life at high rotational speeds, low maintenance costs and operation in vacuum. The usage of standard components and compact bearing electronics have helped lowering the system costs. Nevertheless there is ongoing research aiming at reducing the number of components.

One approach used is the integration of radial and axial bearing components into one unit. This allows a common bias flux [1] or common coils [2] for both force directions. Thus the bearing requires fewer parts and can be built more compact improving both rotor dynamics and system cost.

Another significant challenge arises from operation in vacuum. A rotor running in an air pressure below 10 mbar becomes difficult to cool. Thus even the small rotor losses of a magnetic bearing can lead to overheating. This can be addressed using a stator with minimal slot openings [3] or by minimizing the bias flux [4].

This paper presents a novel magnetic bearing aiming at both problems. Radial and axial force generation is integrated into one unit with a minimal number of poles and coils reducing both rotor losses and system complexity.

2 Integrated Radial-Axial Bearing

The basic structure of the presented bearing is shown in Fig. 1. The front view on the left side shows three teeth with one coil wound on each. It is at first glance quite similar to a three pole heteropolar bearing [5]. The right part of Fig. 1 depicts the side view as a cross section through two of the stator pole tooth. It shows how the three pole heteropolar structure has been extended with a back iron to left. This way an axial bearing can be integrated.

The Fig. 1 denotes the flux caused by the current I_1 while both I_2 and I_3 are zero. The main flux $\Phi_{\mathrm{R}11}$ flows through the pole tooth and enters the rotor trough the radial air gap causing the radial magnetic force $F_{\mathrm{R}11}$. Inside the rotor the flux is divided into three parts: The main part is the axial flux $\Phi_{\mathrm{A}1}$ which leaves the rotor through the axial air gap causing the axial force $F_{\mathrm{A}1}$.

*Contact Author Information: erik.fleischer@tu-dresden.de

A smaller part leaves the rotor through the other radial air gaps as flux Φ_{R12} and Φ_{R13}. Both cause radial forces which partly oppose the main force F_{R11} but are way smaller.

The other two control currents I_2 and I_3 form the same flux path' rotated by 120° and 240° respectively forming the total flux Φ_1, Φ_2 and Φ_3 in each stator tooth. The sum of these

$$\Phi_1 + \Phi_2 + \Phi_3 = \Phi_A. \tag{1}$$

is no longer zero which distinguishes this structure from a three pole heteropolar bearing and results in a greater degree of freedom for the control strategy.

The radial flux Φ_1, Φ_2 and Φ_3 can be controlled freely allowing the operation of the bearing with minimal bias flux and therefore with minimal rotor losses. The axial flux Φ_A can be used for axial control. Since the structure shown in Fig. 1 can only pull the rotor to the left another combined bearing is required on the other end of the rotor to complete the axial suspension.

Nevertheless the structure tightly couples all magnetic fluxes and therefore requires novel approaches to the position control. Therefore this paper presents both a simple linear approach and a more sophisticated nonlinear one based on feedback linearisation.

3 Magnetic Circuit Analysis

As a precondition for the controller design a magnetic circuit model is required. The circuit proposed here consists of only five branches as can be seen in Fig. 2. The first three branches represent each one radial pole tooth. They consist of a magnetic resistance for the air gap $R_{m\delta i}$ and all the iron parts R_{mFeZ}. The air gap resistance can quite accurately described with

$$R_{m\delta i} = \frac{\delta_i}{\mu_0 A_{\delta i}} \quad \text{with} \quad i = 1 \ldots 4 \tag{2}$$

where

$$A_{\delta 1} = A_{\delta 2} = A_{\delta 3} = A_R = A \tag{3}$$

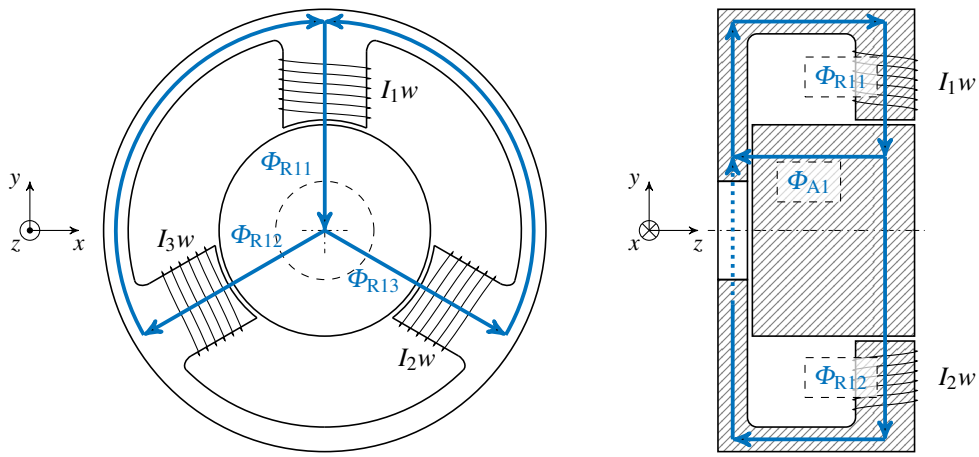

Figure 1: Principle of the combined bearing

represent the cross section of the radial air gaps and

$$A_{\delta 4} = A_{\mathrm{A}} = c_{\mathrm{ax}} A \tag{4}$$

the cross section of the axial one with the cross section ratio c_{ax}.

The resistance of the iron parts is more difficult to calculate. As can be seen in Fig. 1 the magnetic field is a complex three dimensional one. So analytical methods can only give a rough estimation. The approach used here is to trace the flux lines in each part to estimate a medium iron path length and to use the largest cross section along the path as effective iron cross section A_{Fe} in

$$R_{\mathrm{mFe}} \approx \frac{l_{\mathrm{Fe}}}{\mu_{\mathrm{R}}\, \mu_0 A_{\mathrm{Fe}}} \tag{5}$$

to estimate the magnetic resistance of the iron parts. The same approach is used for the axial branch consisting of $R_{\mathrm{m}\delta\mathrm{A}}$ and R_{mFeA} which model the flux flowing through the axial face of the rotor.

This leads to an equation system which fully describes the current-flux relationship in the bearing. Let $\mathbf{R}_{\mathrm{m}} \in R^{4x4}$ be the resistance matrix, $\Phi = [\Phi_1\ \Phi_2\ \Phi_3\ \Phi_{\mathrm{A}}]^{\mathrm{T}}$ the magnetic flux vector, $\mathbf{i} = [I_1\ I_2\ I_3\ 0]^{\mathrm{T}}$ the current vector and the scalar w the number of windings around each pole. The equation

$$w\,\mathbf{i} = \mathbf{R}_{\mathrm{m}} \Phi \tag{6}$$

with

$$\mathbf{R}_{\mathrm{m}} = \begin{bmatrix} R_{\mathrm{m}\sigma}+R_{\mathrm{mFeZ}}+R_{\mathrm{m}\delta 1} & R_{\mathrm{m}\sigma} & R_{\mathrm{m}\sigma} & R_{\mathrm{m}\sigma} \\ R_{\mathrm{m}\sigma} & R_{\mathrm{m}\sigma}+R_{\mathrm{mFeZ}}+R_{\mathrm{m}\delta 2} & R_{\mathrm{m}\sigma} & R_{\mathrm{m}\sigma} \\ R_{\mathrm{m}\sigma} & R_{\mathrm{m}\sigma} & R_{\mathrm{m}\sigma}+R_{\mathrm{mFeZ}}+R_{\mathrm{m}\delta 3} & R_{\mathrm{m}\sigma} \\ R_{\mathrm{m}\sigma} & R_{\mathrm{m}\sigma} & R_{\mathrm{m}\sigma} & R_{\mathrm{m}\sigma}+R_{\mathrm{mFeA}}+R_{\mathrm{m}\delta\mathrm{A}} \end{bmatrix} \tag{7}$$

then describes the magnetic circuit given in Fig. 2.

If the magnetic resistance of the iron and the stray flux is neglected and after substituting for the magnetic resistances according to (3) and (4) one arrives at the equation system

$$\frac{\delta_0}{\mu_0\, c_{\mathrm{ax}} A} \begin{bmatrix} c_{\mathrm{ax}}+1 & 1 & 1 \\ 1 & c_{\mathrm{ax}}+1 & 1 \\ 1 & 1 & c_{\mathrm{ax}}+1 \end{bmatrix} \begin{bmatrix} \Phi_1 \\ \Phi_2 \\ \Phi_3 \end{bmatrix} = w \begin{bmatrix} I_1 \\ I_2 \\ I_3 \end{bmatrix} \tag{8}$$

which is more suitable for analytic studies.

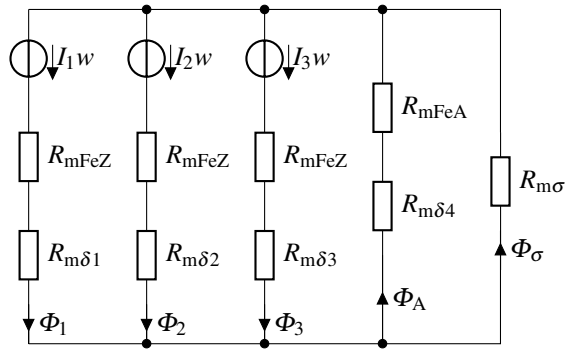

Figure 2: Equivalent magnetic circuit

With the possibility to calculate the resultant flux vector induced by a set of input currents through solving the linear system in (6) or (8) for Φ the forces generated by the magnetic bearing on a rotor can be calculated. Each of the four forces can be expressed with Einstein summation convention by

$$F_i = \frac{{\Phi_i}^2}{2\,\mu_0 A_{\delta i}} \quad \text{with} \quad \Phi_i = R^{-1}_{\mathrm{m}_{ij}} I_j\, w, \quad j = 1\ldots 3, \quad i = 1\ldots 4. \tag{9}$$

These can be mapped on the Cartesian reference frame with

$$\begin{aligned} F_\mathrm{x} &= \frac{\sqrt{3}}{2}(F_2 - F_3) \\ F_\mathrm{y} &= F_1 - \frac{1}{2}(F_2 + F_3) \\ F_\mathrm{z} &= -F_4. \end{aligned} \tag{10}$$

To improve the accuracy of the analytical model, magnetic force measurements were conducted and the results were used to correct the values for the magnetic resistances. More details may be found in [6].

The measurement results also indicated the existence of a significant stray flux Φ_σ. Therefore a stray path with $R_{\mathrm{m}\sigma}$ was introduced into the model and identified from the measurement results.

4 Linear Position Controller

In order to demonstrate that the new bearing can be controlled with minimal computational effort a simple decentral linear controller was designed. A precondition for such a controller is the existence of a controlling quantity with a linear relationship to the bearing force for each bearing axis. Neither winding current exhibits such a behavior. Therefore virtual control currents I_x and I_y are introduced.

Since the arrangement of the three stator poles, which are set 120° apart, is similar to a three phase machine the inverse Clark transformation is a first possibility to calculate the winding currents I_1, I_2 and I_3 from the control currents I_x and I_y in a Cartesian reference frame [5].

$$\begin{bmatrix} I_{\mathrm{c}1} \\ I_{\mathrm{c}2} \\ I_{\mathrm{c}3} \end{bmatrix} = \begin{bmatrix} 0 & 1 \\ \frac{1}{2}\sqrt{3} & -\frac{1}{2} \\ -\frac{1}{2}\sqrt{3} & -\frac{1}{2} \end{bmatrix} \begin{bmatrix} I_\mathrm{x} \\ I_\mathrm{y} \end{bmatrix} \tag{11}$$

$$\mathbf{i}_\mathrm{c} = \mathbf{T}_\mathrm{c}\, \mathbf{i}_\mathrm{xy} \tag{12}$$

The the sum of the resulting currents will always be zero. This is necessary for a heteropolar three pole bearing but the structure presented here with its axial flux does not need this restriction. Therefore a bias current I_0 can be introduced for linearising the force-current relationship.

$$\begin{bmatrix} I_1 & I_2 & I_3 \end{bmatrix}^\mathrm{T} = \begin{bmatrix} I_{\mathrm{c}1} & I_{\mathrm{c}2} & I_{\mathrm{c}3} \end{bmatrix}^\mathrm{T} + I_0 \tag{13}$$

Usually a magnetic bearing is designed for a maximum current I_max because of thermal considerations. If I_x runs from $-I_\mathrm{max}$ to I_max the maximum current is not reached in windings one and two. The bearing is therefore not fully utilized. One can either use a different limit for I_x or change the

transformation matrix as follows.

$$\begin{bmatrix} I_1 \\ I_2 \\ I_3 \end{bmatrix} = \begin{bmatrix} 0 & 1 \\ 1 & -1 \\ -1 & -1 \end{bmatrix} \begin{bmatrix} I_\mathrm{x} \\ I_\mathrm{y} \end{bmatrix} + I_0 \tag{14}$$
$$\mathbf{i} = \mathbf{T}_\mathrm{i}\,\mathbf{i}_\mathrm{xy} + I_0$$

As a side effect the force-current curves become more linear. Additionally the controller calculations are simplified because the winding currents are calculated from the control currents with only a few add and subtract operations.

This control law can be applied to the simplified bearing model in eq. (8) to derive the bearing forces depending on the control currents. Both bearing forces depend on both. If one sets $I_\mathrm{y} = 0$ for F_x and $I_\mathrm{x} = 0$ for F_y the main force-current relationship

$$F_\mathrm{x,x} = \sqrt{3}\,\mu_0\,w^2\,A\,\frac{I_0}{\delta_0^2}\cdot\frac{c_\mathrm{ax}}{c_\mathrm{ax}+3}\cdot I_\mathrm{x} \quad \text{with} \quad I_\mathrm{x}\neq 0 \quad I_\mathrm{y} = 0 \tag{15}$$

$$F_\mathrm{y,y} = \frac{2\,\mu_0\,w^2\,A}{\delta_0^2}\cdot\frac{I_\mathrm{y}^2 + I_0\,c_\mathrm{ax}\,I_\mathrm{y}}{c_\mathrm{ax}+3} \quad \text{with} \quad I_\mathrm{x} = 0 \quad I_\mathrm{y}\neq 0 \tag{16}$$

becomes clear under the assumption that the rotor is at the magnetic center. While the result for F_x is linear, the relationship for F_y contains a quadratic term. Both can be rewritten as follows.

$$F_\mathrm{x,x}^* = \frac{F_\mathrm{x,x}}{F_0} = \frac{\sqrt{3}}{2} I_\mathrm{x}^* \qquad \text{with} \qquad F_0 = 2\,\mu_0\,w^2\,A\,\frac{I_0^2}{\delta_0^2}\cdot\frac{c_\mathrm{ax}}{c_\mathrm{ax}+3} \tag{17}$$

$$F_\mathrm{y,y}^* = \frac{F_\mathrm{y,y}}{F_0} = \frac{I_\mathrm{y}^{*2}}{c_\mathrm{ax}} + I_\mathrm{y}^* \qquad I_\mathrm{x}^* = \frac{I_\mathrm{x}}{I_0} = -1\ldots 1 \tag{18}$$
$$I_\mathrm{y}^* = \frac{I_\mathrm{y}}{I_0} = -1\ldots 1$$

The relative linearity error therefore equals c_ax^{-1}. It follows that the axial air gap cross section area should be at least five times the radial one to get good performance from the linear controller.

The cross coupling in the current-force relationship can be seen if $I_\mathrm{x} = 0$ is set for F_x and $I_\mathrm{y} = 0$ for F_x.

$$F_\mathrm{x,y} = 0 \quad \text{with} \quad I_\mathrm{x} = 0 \quad I_\mathrm{y}\neq 0 \tag{19}$$

$$F_\mathrm{y,x} = -\frac{\mu_0\,w^2\,A}{2\,\delta_0^2}\cdot I_\mathrm{x}^2 \quad \text{with} \quad I_\mathrm{x}\neq 0 \quad I_\mathrm{y} = 0 \tag{20}$$

So there is no cross coupling for F_x and a quadratic one for F_y. This can be transformed into

$$F_\mathrm{y,x}^* = -\frac{(c_\mathrm{ax}+3)}{4\,c_\mathrm{ax}}\cdot I_\mathrm{x}^{*2} \quad \text{with} \quad F_\mathrm{y,x}^* = \frac{F_\mathrm{y,x}}{F_0} \quad \text{and} \quad I_\mathrm{x}^* = \frac{I_\mathrm{x}}{I_0} = -1\ldots 1 \tag{21}$$

showing that the cross coupling force can only be influenced by the cross section ratio c_ax but not significantly.

Because of the nonlinear nature of this cross coupling a linear controller cannot be used for decoupling.

These findings are confirmed by the measurement results in Fig. 4 which were obtained with the prototype shown in Fig. 3 with its the technical data summarized in Tab. 1. Each diagram shows

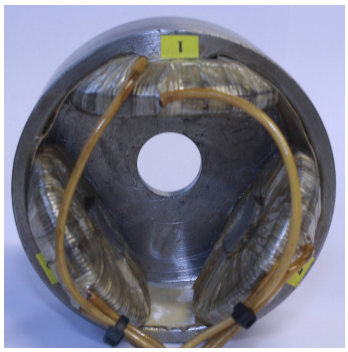

Figure 3: Prototype

Table 1: Technical data of the designed bearing

bore diameter	45 mm
outer diameter	90 mm
axial length	40 mm
nominal flux density	0.8 T
nominal current	5 A
nominal force	74.2 N
cross section ratio c_{ax}	5.8
force/current factor along x-axis	23.8 N A^{-1}
force/current factor along y-axis	27.8 N A^{-1}
force/displacement factor along x-axis	55.5 N mm^{-1}
force/displacement factor along y-axis	55.5 N mm^{-1}

the bearing forces in the x- and y-axes depending on one of the control currents. The measured data points represent actual measured forces and the model data has been calculated based on the magnetic circuit model as shown it Fig. 2 and eq. (6). The cross coupling resulting from I_y in the left diagram of Fig. 4 results from an imperfect centering of the rotor inside the stator during the measurements.

Since the winding currents I_1, I_2 and I_3 are used for the axial control loop as well the control law in (14) has to be extended to include an axial control current I_z. For the combined bearing on the left end of the rotor eq. (14) can be written as

$$\mathbf{i}_L = \mathbf{T}_i \, \mathbf{i}_{xy,L} + I_0 - I_z$$

and for the bearing on the right end of the rotor as

$$\mathbf{i}_R = \mathbf{T}_i \, \mathbf{i}_{xy,R} + I_0 + I_z.$$

Because this technique effectively changes the bias current for, the radial forces I_z should be limited

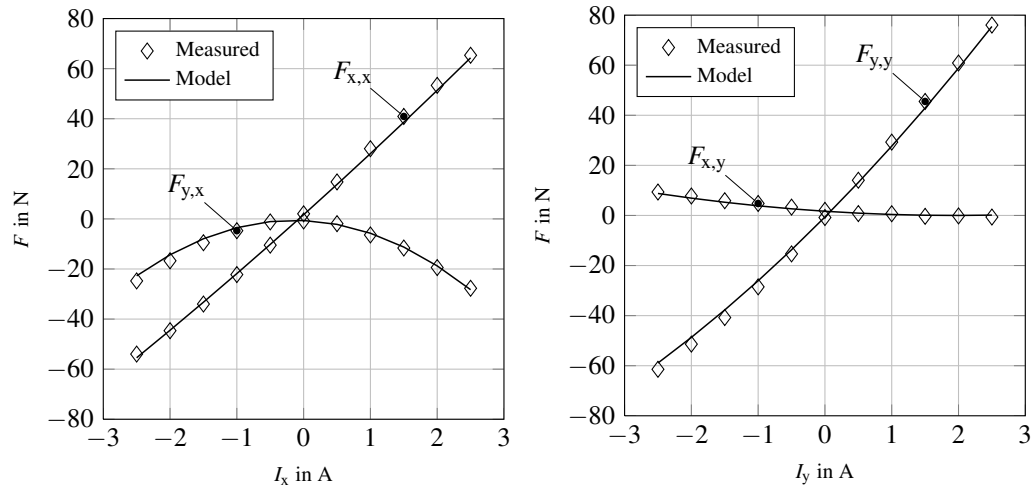

Figure 4: Measured and modelled force-current relationships

to $|I_z| < \frac{1}{3} I_0$ and the winding currents to $0 \leq I_i \leq I_{max}$ in an implementation.

Based on the measured force current curves at different rotor positions both the current/force and force/displacement ratios could be determined for all five control axes and used to design decentral PID controllers for each axis. The bearing stiffness was set to 8 times the natural stiffness and a damping ratio of 0.8 was chosen.

5 Position Control with Minimal Bias Flux

As the bias flux of the bearing is reduced the force-current relation becomes more and more nonlinear hence the controller presented in the last section cannot be used any more. A nonlinear control approach is needed to stabilize the bearing in a low-current working-point. As a quite accurate mathematical model of the bearing exists and has been verified with force measurements a feedback linearisation approach can be used to compensate the nonlinearity. This technique was successfully applied to voltage controlled ([7]) and current controlled ([8]) 3-pole active magnetic bearings. Feedback linearisation gives a linear and controllable system which can easily be stabilized with a PID controller.

As a prerequisite the magnetic model derived in eq. (6) has to be extend by a mechanical model of the rotor. To simplify the Lagrangian dynamic equations of a rigid rotor with mass m we introduce the reduced rotor mass m_{red} for each bearing calculated from the rotor's length $l \in R$, it's moment of inertia in the center of gravity $J_c \in R$ ($J_c = J_{xx} = J_{yy}$) and the lengths $l_1, l_2 \in R$ from the center of gravity to the bearings:

$$m_{red,L} = \frac{m{l_2}^2 + J_c}{l^2} \qquad m_{red,R} = \frac{m{l_1}^2 + J_c}{l^2} \tag{22}$$

Using these as mass points it is possible to retrieve two separate systems of differential equations approximating the rotor dynamics. One combined bearing can be described in state space as

$$\dot{\mathbf{x}} = \mathbf{f}(\mathbf{x}, \mathbf{i}) \tag{23}$$

$$\begin{aligned} \dot{x_1} &= x_2 & \dot{x_3} &= x_4 & \dot{x_5} &= x_6 \\ \dot{x_2} &= \sum_{i=1}^{3} \frac{(R_{m_{ij}}^{-1} I_j w)^2}{2\,\mu_0 A_R\, m_{red}} \sin(\alpha_i) & \dot{x_4} &= \sum_{i=1}^{3} \frac{(R_{m_{ij}}^{-1} I_j w)^2}{2\,\mu_0 A_R\, m_{red}} \cos(\alpha_i) & \dot{x_6} &= \frac{(R_{m_{4j}}^{-1} I_j w)^2}{2\,\mu_0 A_A\, m} \end{aligned} \tag{24}$$

with the state vector $\mathbf{x} = [x\ \dot{x}\ y\ \dot{y}\ z\ \dot{z}]^T$, the input vector $\mathbf{i} = [I_1\ I_2\ I_3\ 0]^T$ and $j = 1 \ldots 4$. The outputs are defined as $y_i = h_i(x) = x_{2i-1}$ with $i = 1 \ldots 3$. The angles α_i define the position of the poles on the stator.

This system is not affine and therefore standard feedback linearisation theory as described in [9] is not applicable. However, [10] describes a method to calculate the relative degree for general SISO (single input single output) systems. This definition can be extended to general MIMO (multiple input multiple output) systems in the form $\dot{\mathbf{x}} = \mathbf{f}(\mathbf{x}, \mathbf{u})$ with m inputs u_i and m outputs $y_i = h_i(\mathbf{x}, \mathbf{u})$ by using the Lie-derivatives and yields

1. $\frac{\partial}{\partial u_j} L_f^k h_i(\mathbf{x}, \mathbf{u}) = 0 \quad$ for all $\quad k < r_i$
2. $A_{ij}(\mathbf{x}) = \frac{\partial}{\partial u_j} L_f^{r_i} h_i(\mathbf{x_0}, \mathbf{u_0})$ is not singular

for the calculation of the relative degree r_i with $i, j = 1 \ldots m$.

Applying this to system (24) gives a relative degree of $r_1 = 2$, $r_2 = 2$ and $r_3 = 2$ and a non singular matrix $A(\mathbf{x}) \in R^{3x3}$. This allows a coordinate transformation to a new state vector $\boldsymbol{\xi}$ which

has $\sum_{i=1}^{m} r_i = 6$ state variables and the components

$$\xi_{ij} = \mathrm{L}_\mathrm{f}^{i-1} h_j(\mathbf{x},\mathbf{i}) \quad \text{with} \quad i = 1 \ldots r \quad \text{and} \quad j = 1 \ldots m. \tag{25}$$

The new linear system with the virtual input $\mathbf{v}$ for one bearing is now

$$\begin{aligned} \dot{\xi_{11}} &= \xi_{21} & \dot{\xi_{12}} &= \xi_{22} & \dot{\xi_{13}} &= \xi_{23} \\ \dot{\xi_{21}} &= \mathrm{L}_\mathrm{f}^2 h_1(\mathbf{x},\mathbf{i}) = \frac{v_1}{m_\mathrm{red}} & \dot{\xi_{22}} &= \mathrm{L}_\mathrm{f}^2 h_2(\mathbf{x},\mathbf{i}) = \frac{v_2}{m_\mathrm{red}} & \dot{\xi_{23}} &= \mathrm{L}_\mathrm{f}^2 h_3(\mathbf{x},\mathbf{i}) = \frac{v_3}{m} \end{aligned} \tag{26}$$

The transformation from virtual input $\mathbf{v}$ to real system input $\mathbf{i}$ is achieved with a control function retrieved by solving the following system for $\mathbf{i}$

$$\mathbf{v}(\mathbf{x},\mathbf{i}) = \begin{bmatrix} \mathrm{L}_\mathrm{f}^2 h_1(\mathbf{x},\mathbf{i})\, m_\mathrm{red} \\ \mathrm{L}_\mathrm{f}^2 h_2(\mathbf{x},\mathbf{i})\, m_\mathrm{red} \\ \mathrm{L}_\mathrm{f}^2 h_3(\mathbf{x},\mathbf{i})\, m \end{bmatrix} = \begin{bmatrix} \sum_{i=1}^{3} \dfrac{(R_{m_{ij}}^{-1} I_j w)^2}{2\mu_0 A_\mathrm{R}} \sin(\alpha_i) \\ \sum_{i=1}^{3} \dfrac{(R_{m_{ij}}^{-1} I_j w)^2}{2\mu_0 A_\mathrm{R}} \cos(\alpha_i) \\ \dfrac{(R_{m_{4j}}^{-1} I_j w)^2}{2\mu_0 A_\mathrm{A}} \end{bmatrix} \tag{27}$$

With a closer look at equation (27) one finds that the virtual inputs are the main axis forces between bearing and rotor $\mathbf{v}(\mathbf{x},\mathbf{i}) = [F_\mathrm{x}, F_\mathrm{y}, F_\mathrm{z}]^\mathrm{T}$. This makes it easy to handle $\mathbf{v}$ as it represents a real physical quantity in the magnetic bearing.

The linear system states x_5 and x_6 are the axial position and velocity of the rotor. Since the two combined bearings at both ends of the rotor share these states it follows that these states must be combined for both bearings. Using the property that the virtual inputs $v_{3,\mathrm{L}}$ of the left bearing and $v_{3,\mathrm{R}}$ of the right bearing represent axial forces on the rotor with opposite directions, one can write for the axial movement

$$\ddot{z} = \frac{v_{3,\mathrm{R}} - v_{3,\mathrm{L}}}{m} \tag{28}$$

and combine it with the equations for radial states $\dot{\xi_{11}}$, $\dot{\xi_{21}}$, $\dot{\xi_{21}}$, $\dot{\xi_{22}}$ of the linear system in eq. (26). Introducing the input $v_\mathrm{axial} = v_{3,\mathrm{R}} - v_{3,\mathrm{L}}$ gives a system $\dot{\tilde{\xi}} = \tilde{\mathbf{f}}(\mathbf{x},\tilde{\mathbf{v}})$ with five equations, five virtual inputs and five outputs. This system reduction leads to the mapping

$$\tilde{\mathbf{v}} = [v_{1,\mathrm{L}}\ v_{1,\mathrm{R}}\ v_{2,\mathrm{L}}\ v_{2,\mathrm{R}}\ v_\mathrm{axial}]^\mathrm{T} \mapsto \mathbf{v} = [v_{1,\mathrm{L}}\ v_{1,\mathrm{R}}\ v_{2,\mathrm{L}}\ v_{2,\mathrm{R}}\ v_{3,\mathrm{L}}\ v_{3,\mathrm{R}}]^\mathrm{T} \tag{29}$$

which is a under-determined relation. Therefore the equations $\mathbf{i}(\mathbf{x},\tilde{\mathbf{v}})$ will be under-determined too.

The simple structure of the linear mathematical model $\dot{\tilde{\xi}} = \tilde{\mathbf{f}}(\mathbf{x},\tilde{\mathbf{v}})$ makes it immediately clear that there exists a one to one relation of input $\tilde{v}_i$ to output y_i. Uncoupled systems like this can be stabilized by independent controllers. Therefore five PID controllers are designed in a way that each decoupled part behaves like a damped mass-spring system. From given stiffness and damping values it is possible to directly get the controller parameters.

The virtual inputs as calculated by the PID controllers are transformed to real system inputs by equation (27). This is a non trivial calculation as the equation system $\mathbf{i}(\mathbf{x},\tilde{\mathbf{v}})$ is nonlinear and under-determined. A standard approach would be the Newton-Raphson method. On a embedded device operating in real time an iterative algorithm is not applicable. A algorithm to approximate the solution in an appropriate time is presented. It uses the physical relation that virtual inputs are the

main axis forces $\tilde{\mathbf{v}}(\mathbf{x},\mathbf{i}) = \mathbf{F}_{\text{main}}$.

The first step is to calculate the minimal pole forces F_1, F_2 and F_3 needed to generate the radial main forces F_x and F_y as described in [11]. The mapping from pole to main forces as described by equation (10) is a under-determined equation system and therefore it is possible to choose F_1 freely and then calculate the remaining pole-forces with equation (10). This yields

$$F_1 = \begin{cases} 0 & \text{if} \quad F_\text{y} < \dfrac{|F_\text{x}|}{\sqrt{3}} \\ F_\text{y} + \dfrac{|F_\text{x}|}{\sqrt{3}} & \text{else} \end{cases} \qquad F_2 = F_1 - F_\text{y} - \frac{F_\text{x}}{\sqrt{3}} \qquad F_3 = F_1 - F_\text{y} + \frac{F_\text{x}}{\sqrt{3}} \tag{30}$$

and is an exact solution for the radial forces. Because of the bearing topology a radial flux always implies an axial one and therefore the radial forces always imply an axial force. From the magnetic circuit in Fig. 2 we get the mesh equation

$$0 = R_{\text{m}\sigma}\Phi_1 + R_{\text{m}\sigma}\Phi_2 + R_{\text{m}\sigma}\Phi_3 + (R_{\text{m}\sigma} + R_{\text{mFeA}} + R_{\text{m}\sigma\text{A}})\Phi_4 \tag{31}$$

in which eq. (9) can be used to substitute for Φ to get

$$F_{4\,\text{imp}} = \frac{\pm\sqrt{F_1} \pm \sqrt{F_2} \pm \sqrt{F_3}}{k} \quad \text{with} \quad k = \frac{R_{\text{m}\sigma} + R_{\text{mFeA}} + R_{\text{m}\sigma\text{A}}}{R_{\text{m}\sigma}} \sqrt{\frac{A_\text{A}}{A_\text{R}}} \tag{32}$$

which can be used to calculate the minimal implied axial force $F_{4\,\text{imp}}$.

Note that the forces are always directed toward the poles. Nonetheless the calculation yields an undetermined sign for each force in (32). This is due to the fact that the flux Φ_i can have two directions (into or out of the rotor) for the same force F_i. The sign of Φ_i of needs to be propagated through to make the balance valid. To determine the right sign one has to know the flux directions and therefore the current directions.

With the knowledge of the minimal implied axial forces of each bearing it is possible to use the systems under-determination to control the resulting axial force. The given axial force $v_\text{axial} = F_\text{z}$ can be achieved with any valid combination of $v_{3,\text{L}} = F_{4,\text{L}}$ and $v_{3,\text{R}} = F_{4,\text{R}}$. Which axial force has to be increased and by which amount can be calculated with $F_\Delta = (F_{4\,\text{imp,R}} - F_{4\,\text{imp,L}})$ by

$$F_{4,\text{L}} = \begin{cases} F_{4\,\text{imp,L}} & \text{if } F_\Delta < F_\text{z} \\ F_{4\,\text{imp,L}} + F_\Delta - F_\text{z} & \text{if } F_\Delta \geq F_\text{z} \end{cases} \qquad F_{4,\text{R}} = \begin{cases} F_{4\,\text{imp,R}} & \text{if } F_\Delta \geq F_\text{z} \\ F_{4\,\text{imp,R}} + F_\text{z} - F_\Delta & \text{if } F_\Delta < F_\text{z} \end{cases} \tag{33}$$

Now for each Bearing the three minimal radial forces and the required axial force are known. At this stage the calculations for one of the bearings are complete, as its axial force remains the minimal one as stated by (33). For the other bearing the balance equation (32) is not fulfilled any more, as the axial force was increased without changing the radial components. To re-balance the forces one can use the fact that the radial forces can be increased all by a the same amount F_0 without changing the resultant main forces F_x and F_y. This can be expressed as

$$0 = \pm\sqrt{F_1 + F_0} \pm \sqrt{F_2 + F_0} \pm \sqrt{F_3 + F_0} \pm \sqrt{F_4} k \tag{34}$$

and then be solved for F_0. This is a smaller nonlinear problem than the original system (27). However it requires an iterative solving approach as well. To circumvent this we use the linear Taylor approximation for square roots around $F_{0_{k-1}}$ which is the value of F_0 from the previous calculation.

For $f(F_0) = \sqrt{F_1 + F_0}$ this gives

$$T(F_0) = f(F_{0_{k-1}}) + f'(F_{0_{k-1}})(F_0 - F_{0_{k-1}}) = \sqrt{F_1 + F_{0_{k-1}}} + \frac{1}{2\sqrt{F_1 + F_{0_{k-1}}}}(F_0 - F_{0_{k-1}}) \tag{35}$$

Replacing all square roots in (34) in the same manner as (35) and introducing $\tilde{F_1} = F_1 + F_{0_{k-1}}$ etc. the resultant force vector F_{res} can be calculated by

$$F_0 = \frac{\pm\sqrt{\tilde{F_1}} \pm \sqrt{\tilde{F_2}} \pm \sqrt{\tilde{F_3}} \pm \sqrt{F_4}k}{\mp\frac{1}{2\sqrt{\tilde{F_1}}} \mp \frac{1}{2\sqrt{\tilde{F_2}}} \mp \frac{1}{2\sqrt{\tilde{F_3}}}} + F_{0_{k-1}} \qquad F_{\text{res}} = \begin{bmatrix} F_1 + F_0 \\ F_2 + F_0 \\ F_3 + F_0 \\ F_4 \end{bmatrix} \tag{36}$$

With all forces known for both bearings one can calculate the winding currents with

$$\Phi_i = \sqrt{2\mu_0 A_i F_{\text{res},i}} \qquad w\mathbf{i} = \mathbf{R}_{\text{m}}\Phi \tag{37}$$

Note that the forces are always positive and the current directions have to be used as defined for equation (32).

6 Simulation Results

To verify and optimize the proposed control schemes simulations have been carried out. A complete 5-axis suspension with a stiff rotor has been modelled using the magnetic circuit model as outlined in Fig. 2 and eq. (6). The rotor was suspended horizontally with the gravity pointing down the y-axis. The PID controllers were implemented as using the discrete PITD$_2$-algorithm with a sampling rate of 21.3 kHz.

Both control schemes were tested using a 10 µm step on the reference signal on either the x-axis and the y-axis. The results achieved with the linear control scheme are shown in Fig. 5 and demonstrate that the control scheme can be used to stabilize the proposed bearing structure. In the step response for the x-axis a small movement of 1.9 % of the step distance along the y-axis can be seen. This is caused by the cross coupling derived in eq. (20).

While the x-axis step did have little effect on the z-axis, the z-axis step response shows a significant effect of the z-axis movement on the y-axis which carries the rotor weight and has therefore a non-zero control current. The z-axis controller effectively changes the bias for the radial forces and therefore changes the force-current ratio and in turn causes a disturbance on the y-axis.

These effects can be solved by applying the feedback linearisation as is demonstrated by the step responses in Fig. 6. These show no significant effects of cross coupling. What is more the nonlinear control scheme shows nearly the same performance as the linear controller while requiring much less magnetic bias.

7 Conclusion and Outlook

A new magnetic bearing structure which combines both radial and axial force generation in one compact unit has been presented. The proposed magnetic circuit model has been verified by force measurements and is used to design both a linear and a nonlinear control scheme. It has been shown that the bearing can be linearised quite well with the introduction of a bias current. Although there remains some coupling between the bearing axes the system shows good performance. The only

notable exception is the cross coupling of the axial bearing control loop on the radial ones. It acts as a significant disturbance on the radial axes and must therefore be limited in its performance.

The second proposed control scheme clearly demonstrates that these limitations can be overcome with a feedback linearisation approach. Additionally this allows minimizing the magnetic bias and in turn both stator and rotor losses.

Further efforts will concentrate on finishing the test rig which then can be used to verify the presented control schemes at standstill and up to the nominal speed of 30 000 rpm.

So far the linear control scheme is based on an empiric approach to determine the transformation matrix between the control currents and the winding currents. It is planned to study more systematic approaches as outlined for example in [12] which may allow the inclusion of the axial axis into the linearisation scheme.

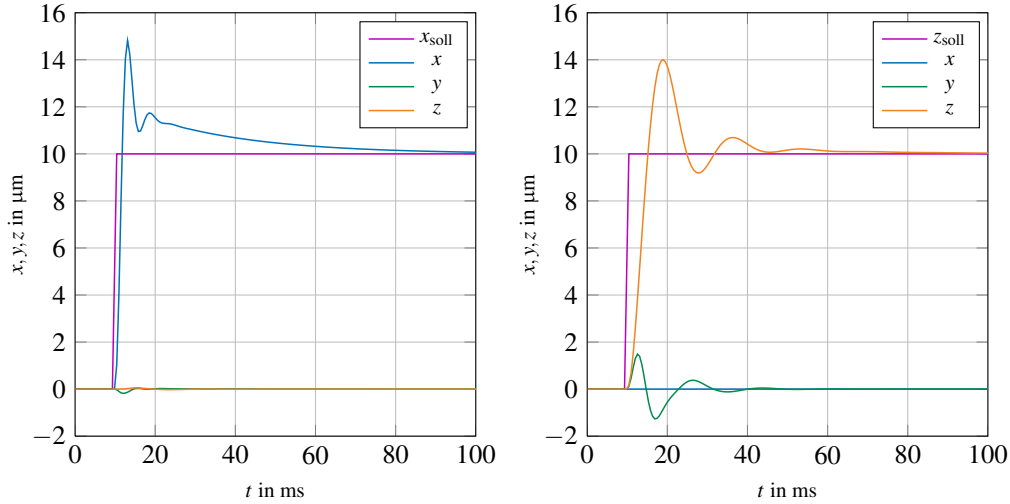

Figure 5: Simulated step responses with linear control

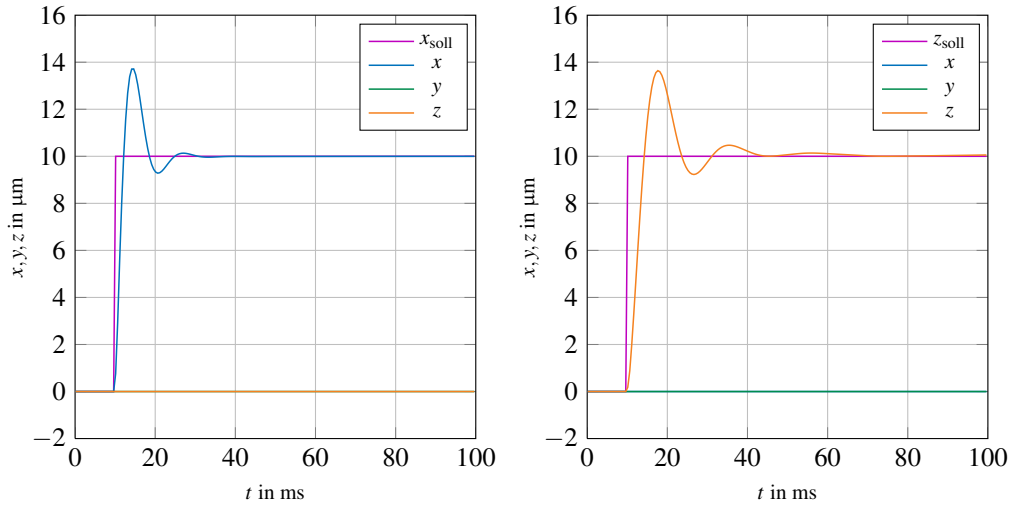

Figure 6: Simulated step responses with nonlinear control

As implemented now the feedback linearisation is based on the full model which sets high demands on the controller hardware. It can be assumed that this is not necessary to reach a good controller performance. Therefore further studies will try to find an optimal balance between computational effort and controller performance.

Acknowledgement

The authors would like to thank the DFG (Deutsche Forschungsgemeinschaft) for funding this project.

References

[1] F. Betschon, 'Design principles of integrated magnetic bearings', Dissertation, ETH Zürich, 2000.

[2] M. Reisinger, H. Grabner, S. Silber, W. Amrhein, C. Redemann and P. Jenckel, 'A novel design of a five axes active magnetic bearing system', in *Twelfth International Symposium on Magnetic Bearings*, 2010.

[3] N. Kurita, R. Kondo and Y. Okada, 'Lossless magnetic bearing by mean of smoothed flux distribution', in *Ninth International Symposium on Magnetic Bearings*, Lexington, Aug. 2004.

[4] M. Kasarda, P. Allaire, P. Norris, C. Mastrangelo and E. Maslen, 'Experimentally determined rotor power losses in homopolar and heteropolar magnetic bearings', *Journal of Engineering for Gas Turbines and Power*, vol. 121, no. 4, pp. 697–702, Oct. 1999, ISSN 0742-4795.

[5] W. Hofmann, 'Behaviour and control of an inverter-fed three-pole active radial magnetic bearing', in *Industrial Electronics, 2003. ISIE '03. 2003 IEEE International Symposium on*, vol. 2, 2003, 974–979 vol. 2. [Online]. Available: `http://ieeexplore.ieee.org/xpls/abs_all.jsp?arnumber=1267954`.

[6] E. Fleischer, S. Tröger and W. Hofmann, 'Development of an active magnetic bearing with a soft magnetic composite core', in *Proceedings of the International Conference Magnetism and Metallurgy*, Jun. 2012.

[7] L. Li and J. Mao, 'Exact linearisation of a magnetic bearing actuators for a uniform upper bound of force slew rate', *IEEE Transactions on Control Systems Technology*, vol. 5, pp. 587–597, 1999.

[8] C.-T. Hsu and S.-L. Chen, 'Nonlinear Control of a 3-pole active magnetic bearing system', *automatica*, vol. 39, pp. 291–298, 2003.

[9] A. Isidori, *Nonlinear Control Systems*. New York: Springer-Verlag, 1989. [Online]. Available: `http://www.bibsonomy.org/bibtex/25d0f70e71e2c423117ac88d97679920a/jmm`.

[10] M. A. Henson and D. E. Seborg, *Nonlinear process control*. Prentice Hall, 1997, p. 432.

[11] S. Eckhardt and J. Rudolph, 'High precision synchronous tool path tracking with an amb machine tool spindle', in *Ninth International Symposium on Magnetic Bearings*, 2004.

[12] E. H. Maslen and D. C. Meeker, 'Fault tolerance of magnetic bearings by generalized bias current linearization', *IEEE Trans. Magn.*, vol. 31, no. 3, pp. 2304–2314, 1995. DOI: `10.1109/20.376229`.